CHARACTERIZING POLAR LAYERED DEPOSITS AT THE MARTIAN NORTH POLE: AN ASSESSMENT OF LOCAL VARIATIONS. S. M. Milkovich and J. W. Head, III, Dept of Geological Sciences, Brown University, Providence, RI 02912. Sarah_Milkovich@brown.edu

Introduction: Within the northern residual polar cap of Mars are dark lanes or troughs; on the walls of these exposures are layered deposits. These deposits consist of extensive lateral layers of ice and dust and are found throughout the polar cap. They were first identified in Mariner 9 images [1, 2] and later studied in detail with the Viking orbiters [e. g. 3, 4, 5, 6]. In these images, the layers appear to consist of alternating sequences of light and dark layers ~ 5 to 25 m thick [4, 5].

Recent data taken by the Mars Orbiter Camera (MOC) onboard the Mars Global Surveyor (MGS) reveal that the layers are thinner and more numerous than Viking images suggested. Layers are seen with thicknesses at the limit of resolution (~2 m) and it is possible that smaller scale layers may also exist [7]. The individual layers show considerable variation in thickness, ranging from several meters (the limit of resolution) to several tens of meters [8]. Some layers are observed to pinch out [7]. Additionally, layers show varying resistance to erosion. In particular, a "marker bed" 20 m thick with resistant knobs ~ 10 m wide is observed in many places [7, 9, 10].

Layers also show variation in surface texture. Individual layers display surfaces with pockmarks, brick-like textures, and a pattern similar to a deformed, woven structure [8]. It is not clear if the textures are a property of the layer or are limited to the exposed surface. There is not a relation between texture and location. The variety of textures may be due to structural properties of the individual layers which caused different amounts of erosion [8]. Some textures indicate a pitted surface, which may be due to outgassing of clathrate-rich layers [10].

These layers are laterally extensive. Several images taken from a single trough in Figure 1 show that in some regions individual layers can be traced for many hundreds of kilometers [7, 10]. Two different investigators have proposed that the marker bed can be found in multiple troughs 50 km apart [7, 9]. However, a preliminary assessment of images found that layer sequences vary greatly around the cap [8]. An additional difficulty for comparing image sequences is the seasonal surface frost deposits found throughout this area. Indeed, two sequences can look very different from each other when in reality they are taken from either side of the same image [10]. Frost can cause several layers to look like one thick layer. It can also be preferentially deposited within a segment of a dark region, revealing many layers in an area which would otherwise be thought to be one layer [10].

Many models were proposed for the formation of these deposits based on Viking data [e.g., 11, 5] but the details of the formation process remain unknown. The main driving force behind the deposits is thought to be episodic climate variations due to orbital cycles. Indeed, some effort has been made to connect layers to specific orbital cycles, especially obliquity, using computer models [4, 12] and spectral signal analysis [13]. However, the variability of individual layers may indicate the influence of smaller scale variations. Such variations may include the influence of local topography or non-uniform deposition of material such as ejecta from major impacts or pyroclastic material [8]. Additionally, the thinner layers may indicate that the martian climate produces deposits on timescales less than the obliquity cycle [7]. Thus, characterization of cycles within layers without relying on specific orbital periods is a necessary first step before introducing process-specific factors.

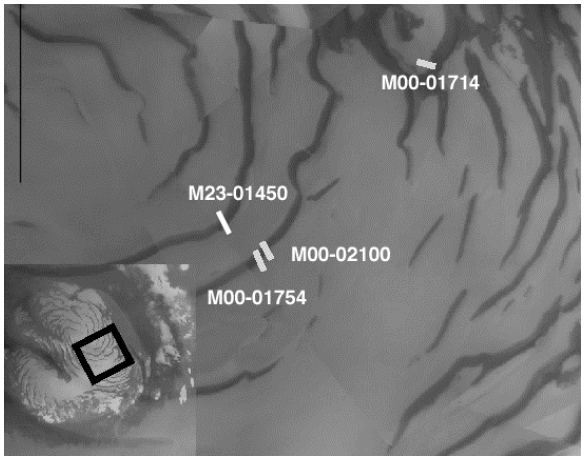

Fig. 1. Location of troughs and images in the northern cap under study.

An understanding of the formation processes of the polar layered terrain will provide insights into the processes of trough formation, lateral propagation, erosion, and deposition. It will also allow us to interpret the simple vertical record of climate change encoded in the layered deposits. Ultimately, we will gain a foundation upon which we can build a better model for the interactions of the various volatile deposits on Mars, including the current polar surface as well as the latitude-dependent layer of subsurface ice currently being mapped by Mars Odyssey [14, 15].

In order to begin this foundation of knowledge we first must characterize sections of layers and quantitatively compare the layer sequences in one trough with another. In this way, constraints may be placed on trough formation mechanisms.

Characterization Using Fourier Analysis: One-dimensional Fourier analysis is used to break a complex signal down into sine and cosine components [16]. Dominant wavelengths of the complex signal can be measured from these components. The polar layered deposits record a complex signal of changing depositional environments in their layers. FFTs may be a valuable tool to characterize how the depositional environment varied from location to location.

The Fourier transform is described by the following equation:

$$F(k_x) = \int_{-\infty}^{\infty} f(x) e^{-ik_x x} dx \qquad (1)$$

where $k_x=2\pi/\lambda$ is the spatial wavenumber. Spatial frequency, $k_x/2\pi$, can be inverted to find spatial wavelength, $\lambda=2\pi/k_x$. The power spectrum of the signal is described by:

$$P(k_x) = \int_{-\infty}^{\infty} \left|F(k_x)\right|^2 dk_x \qquad (2)$$

A fast Fourier transform (FFT) is a discrete form of equation (1) and is computed numerically. Plots of spatial frequency vs. relative power were created using the FFT function in the Matlab package software; these plots were then inverted to determine spatial wavelengths. The same method and program were used as is described in [16].

Applying FFTs to the PLD: This analysis compares the FFTs of DN profiles from multiple images. First, images are calibrated and the associated MOLA data retrieved using programs from the ISIS image processing package. The MOLA data is interpolated between shots to provide an elevation value for each pixel of the image. Thus, the exposure of layers in the image is projected back onto the vertical wall of the trough. The DN profile is then adjusted to run perpendicular to the layer margins. Next this data set is adjusted so that it consists of DN values at locations spaced evenly down the vertical wall. This process interpolates between DN values for neighboring pixels; while this may not be a true assumption at the boundaries between layers, the pixel size is small (1.8 m/pxl) that the errors introduced are negligible. The interpolations were done using the Arand suite of programs developed at Brown University for paleoceanographic studies. Evenly spaced data is required for the FFT process; the adjusted data is then run through the Matlab FFT program.

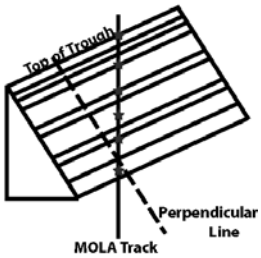

Fig. 2 Method for rectifying images.

To be a useful tool for comparing images, FFTs must return similar results from layer sequences which are practically identical. Previously, we have performed FFT analysis on many calibrated but not slope-corrected profiles from a single image, M00-01754. Profiles from either side of this image yielded very similar dominant wavelengths, as was expected. However, the dominant wavelength varied down the length of the trough wall exposure. This may be due to compression of the layers towards the base of the deposit from the overlying material or to a change in the depositional environment [17]. The first steps in the current analysis were discussed in [18]; this abstract is a continuation of that study.

Results: The analysis described above was carried out on 4 images in 3 troughs (Figure 1). Each image was taken during the same season to reduce the effect of surface frost on the layers (Table 1). The FFT results for two of the images are found in Figures 3 and 4.

Table 1: Image Information

Image Number	Resolution	Ls	Sun Angle
M00-01714	1.81 m/pxl	122.82˚	304˚
M00-01754	1.81 m/pxl	122.89˚	123˚
M00-02100	1.81 m/pxl	123.86˚	127˚
M23-01450	12.1 m/pxl	106.49˚	74˚

Long range wavelengths show a dominant peak ranging from 27 to 33 m; this wavelength can also be seen in the DN profiles themselves. This wavelength range is influenced by packets of multiple layers.

Mid range wavelengths, on the other hand, are influenced by individual layer thickness. Two images 60 km apart in the same trough, M00-02100 and M00-01754, have different wavelengths in this range which indicates that the thicknesses are changing non-systematically in a single trough. This result can also be seen in a direct comparison of the profiles. It indicates that deposition varies on a very local scale to cause layer thicknesses to change within 60 km. This

result will be compared with a similar analysis of multiple images in the trough immediately to the north.

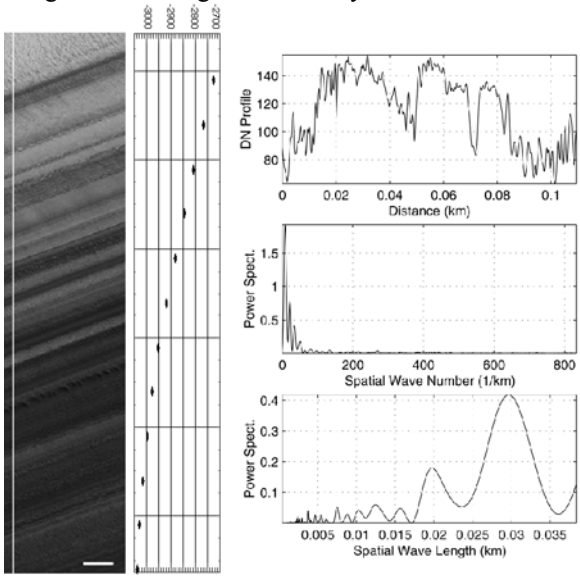

Fig. 3 FFT results for image M00-01754. Scale bar is 200 m.

Future work will cross-correlate the results of the FFT analysis to quantitatively compare dominant wavelengths from each image

Discussion: Laskar et al [13] recently used spectral analysis to examine image M00-02100. They visually identified a cyclic pattern (~80 m/cycle) in the DN profile of the upper portion of this image. They correlated the first three of these cycles with calculated insolation patterns up to ~500,000 years and calculated a deposition rate for the entire cap of 0.05 cm/yr. When we examine the DN profile of image M00-01714 we do not observe the cyclic pattern identified in M00-02100. If insolation is having consistant effects, we should be able to find such a pattern in all images in this region. However, we do find a consistant signal on smaller wavelengths (~30 m) in all images studied up to this point. This would result in a deposition reate of 5.4-6.4 x 10^{-3} cm/yr. The purpose of this calculation is not to arrive at a deposition rate for the cap, but rather to demonstrate the range of results possible when interpreting images without thoroughly characterizing them first.

In this region we have examined 4 images from 3 troughs and examined their DN profiles and dominant wavelengths. We find a dominant wavelength of ~ 30 m in all images; this may be related to the climatic forcing process. We also see that individual layer thicknesses change non-systematically in a single trough. The profiles provide more details of the differences between layers, but the FFTs provide a useful, quantitative overview for comparing data.

Characterization of the layered deposits is key to our understanding of the processes which shape the polar regions and the martian climate as a whole. Fourier analysis provides a useful tool to assist in comparisons of layer sequences. Additionally, Fourier analysis will allow us to pull out the cycles within these sequences which can then be used to constrain the processes which deposited these layers and shaped the troughs. These efforts in turn will aid our understanding of the martian climate system.

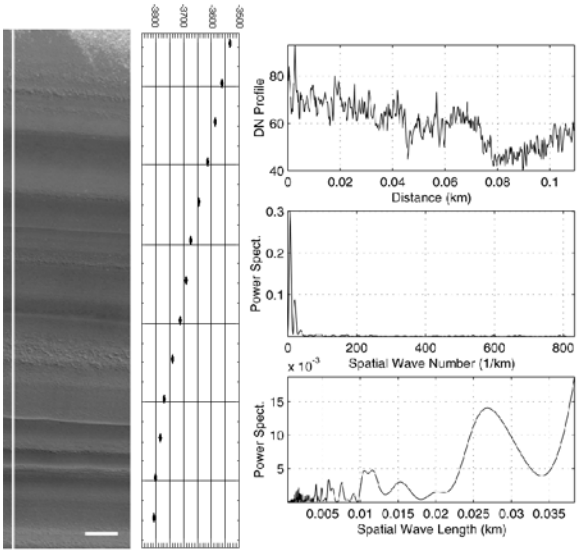

Fig. 4 FFT results for image M00-01714. Scale bar is 200 m.

Acknowledgments: *Thanks are extended to Misha Kreslavsky for helpful discussions, and to Timothy Herbert and Phillip Howell of Brown University for help with computer programs.*

References: [1] Soderblom L., et al. (1973) *JGR 78,* 4197-4210. [2] Cutts J. A. (1973) *JGR 78*, 4231-4249. [3] Kieffer H. H. et al, (1976) *Science 194*, 1341-1344. [4] Blasius K. R., et al. (1982) *Icarus 50*, 140-160. [5] Howard A. D., et al. (1982) *Icarus, 50,* 161-215. [6] Thomas P. C. et. al. in *Mars* [ed.by H. H. Kieffer et al] pp.767-795. Univ. of Arizona Press, Tuscon. [7] Malin M. C., Edgett K. S. (2001) *JGR 106*, 23429-23570. [8] Milkovich, S. M., Head J. W. (2001) LPSC 32, #1976. [9] Kolb E. J., Tanaka K. L (2001) *Icarus 154,* 22-39. [10] Milkovich, S. M., Head, J. W. (2002) LPSC 33, 1713. [11] Squyres, S. W. (1977) *Icarus 40,* 244-261. [12] Cutts, J. A., Lewis, B. H. (1982) *Icarus50,* 216-244. [13] Laskar, J., et al. (2002) *Nature 419,* 375-377. [14] Mitrofanov, I. et al (2002) *Science 297,* 78-81. [15] Boynton, W. V. et al (2002) *Science 297,* 81-85. [16] Patel, J. G., et al (1999) *JGR 104*, 24057-24074. [17] Milkovich, S. M., Head J. W. (2002) Microsymposium 36, #ms069. [18] Milkovich, S. M., Head J. W. (2003) LPSC 34, 1342.